

# Soft Matter

Accepted Manuscript



This is an *Accepted Manuscript*, which has been through the Royal Society of Chemistry peer review process and has been accepted for publication.

*Accepted Manuscripts* are published online shortly after acceptance, before technical editing, formatting and proof reading. Using this free service, authors can make their results available to the community, in citable form, before we publish the edited article. We will replace this *Accepted Manuscript* with the edited and formatted *Advance Article* as soon as it is available.

You can find more information about *Accepted Manuscripts* in the [Information for Authors](#).

Please note that technical editing may introduce minor changes to the text and/or graphics, which may alter content. The journal's standard [Terms & Conditions](#) and the [Ethical guidelines](#) still apply. In no event shall the Royal Society of Chemistry be held responsible for any errors or omissions in this *Accepted Manuscript* or any consequences arising from the use of any information it contains.

# Evidence of random copolymer adsorption at fluctuating selective interfaces from Monte-Carlo simulation studies

Igor Gazuz<sup>\*,†</sup> and Jens-Uwe Sommer<sup>‡</sup>

*Leibniz-Institut für Polymerforschung Dresden e. V. , 01069 Dresden, Germany, and Technische Universität Dresden, Institut für Theoretische Physik, 01062 Dresden, Germany*

E-mail: gazuz@ipfdd.de

## Abstract

We perform Monte Carlo simulations of a binary, strongly separated mixture of A- and B-type homopolymers with some amount of random AB copolymers added. The interface is analyzed and the interface tension is calculated using the model of capillary waves. We can clearly demonstrate that random copolymers are localized at real, fluctuating interfaces between incompatible polymer species and micellization is not favored over adsorption. Our study proves that random copolymers are potential candidates for compatibilization of polymer-polymer mixtures. By simulating random copolymers in a one-component bulk and comparing their free energy to the copolymers adsorbed at the two-phase interface we show that the adsorption is thermodynamically stable. We use scaling arguments developed for ideal and non-fluctuating interfaces to rationalize the simulation results and we calculate the reduction of interface tension with increasing amount of the adsorbed copolymers.

---

\*To whom correspondence should be addressed

<sup>†</sup>Leibniz-Institut für Polymerforschung Dresden e. V. , 01069 Dresden, Germany

<sup>‡</sup>Technische Universität Dresden, Institut für Theoretische Physik, 01062 Dresden, Germany

# 1 Introduction

Behavior of AB copolymers at the interface between two immiscible homopolymer species A and B has been in the focus of study already for a long time. It was shown experimentally<sup>1-5</sup>, in theoretical<sup>6-13</sup> and simulation<sup>11-23</sup> studies that copolymers tend to adsorb at the interface. Adsorbed copolymers can be used in technological applications like the compatibilization and mechanical reinforcement of composite materials.

Especially the case of random AB copolymers attracted much interest since these are easy to synthesize and should exhibit rather good properties as compatibilizers, in particular to reinforce AB composites by forming entanglements across the interface. Up to now, theoretical as well as simulation studies of random copolymers at interfaces were limited to considering ideal, non-fluctuating interfaces. These were modeled by a step potential preferring either the A or the B species depending on the side of the interface, and both phases represented athermal solvent for both monomer species. The mechanism of adsorption of random copolymers at ideal interfaces was shown to be governed by the formation of so called “excess blobs”<sup>7,8</sup>. These are chain parts containing an excess of one species, which is localized at the preferred side of the interface. The corresponding scaling variable can be inferred<sup>6</sup> from a simple Imry-Ma type argument<sup>24</sup>. The latter is based on the fact that a fragment of a random copolymer containing  $g$  monomers will have a random excess of  $g^{1/2}$  monomers of one species. This leads to a scaling variable that can be chosen as  $\chi N^{1/2}$ , where  $\chi$  is the Flory-Huggins parameter representing the selectivity of the interface and  $N$  is the chain length. The corresponding power laws for the asymptotic scaling of the radius of gyration and for the order parameter of the adsorption were derived and tested by simulations in Refs.<sup>16,18</sup>. In further works the effect of asymmetric interface potentials<sup>20</sup> or interface layers<sup>23</sup> and effects occurring when many chains are adsorbed<sup>21,22</sup> were considered.

The validity of the results obtained for ideal interfaces for the case of real interfaces was however challenged<sup>25</sup> on the grounds that copolymers build micelles in the bulk<sup>26</sup> and it was claimed that the micellar state might be thermodynamically more favorable than the adsorbed state at the interface. In the present study, we model the immiscible phases directly and thus allow for the

formation of a real, fluctuating interface. We are thus able to study the properties of the interface itself, in particular the surface tension depending on the amount of the adsorbed copolymers. We also test the validity and applicability of the theoretical predictions made for random copolymers at ideal interfaces for the case of fluctuating interfaces. Furthermore, the presence of explicit bulk phases allows us to test the competition between the micellar state and interface localization. From the monomer densities in the bulk and at the interface a conclusion that the preferred state for the random copolymers is the adsorbed one already can be done. We also simulate random copolymers in one phase and compare the free energy of the micelles, which copolymers build in this case with the free energy of the copolymers adsorbed at the two-phase interface. This allows us to show that the interface adsorption is definitely thermodynamically favored by random copolymers.

The rest of this work is organized as follows. After the description of our simulation model in section 2 we consider the distribution and single chain properties of random copolymers at AB-surface in Section 3.1. In Section 3.2, the surface tension of the interface is studied. In Section 3.3, the scaling laws based on the excess blob concept are reconsidered for real fluctuating interfaces. The free energy for adsorbed and non-adsorbed random copolymers is calculated in Section 3.4. Our conclusions are presented in Section 4.

## 2 Simulation model

We employ a version of the bond fluctuation model (BFM)<sup>27</sup>, which was described in detail elsewhere<sup>28</sup>. In general during a Monte Carlo move, excluded volume conditions and bond restrictions are checked and a move is only carried out if the lattice places for the moved monomer are free and the new bonds are within the set of allowed (108) bond vectors. Additional interactions between the monomers are taken into account using a Metropolis algorithm. In the present case the interaction energy is determined by the number of AB-contacts within a range of nearest neighbor positions around a given monomer. As in previous work<sup>28,29</sup> we consider only repulsive interactions between unlike species which avoids unphysical freezing effects even in the case of strong

segregation. By counting the number of AB contacts on the lattice, three constellations with 4, 2 and 1 contacts have to be distinguished. They occur with probability  $h_I = 0.18$ ,  $h_{II} = 0.48$  and  $h_{III} = 0.34$ , respectively<sup>28</sup>. Thus the average interaction energy of an AB monomer pair is given by

$$E_{AB} = \varepsilon(4h_I + 2h_{II} + h_{III}) = 2.02\varepsilon, \quad (1)$$

where  $\varepsilon$  denotes a microscopic interaction parameter per lattice contact which is the primary parameter in the simulation model. The Flory-Huggins parameter<sup>30</sup> is related to  $E_{AB}$  by

$$\chi = \frac{p_{eff}E_{AB}}{k_B T}, \quad (2)$$

where  $p_{eff} \approx 3.5$  is the effective coordination number of the monomer in our simulations. Using Equation (1) we obtain the approximate relationship

$$\chi \approx \frac{7\varepsilon}{k_B T}. \quad (3)$$

In the following we consider energy units given by  $k_B T \equiv 1$ .

The simulation box has  $L \times L \times D$  lattice points with the parallel extension  $L = 256$  and the perpendicular extension  $D = 64$ . We apply periodic boundary conditions in each direction. The A and B homopolymers (referred to as bulk in the following) have the chain length (number of monomers) of  $N_h = 64$ . We consider random A-B copolymers (referred to as RCP in the following) of different chain lengths  $N = 16, 32, 64, 128$ . We denote the total number of random copolymers by  $n_c$ .

The preparation of the system is as follows. First, an athermal mixture of  $n_c$  homopolymers of length  $N$  and a certain amount  $n_h$  of homopolymers with length  $N_h$  is prepared such as to obtain the lattice occupation fraction of 0.5, corresponding to a dense melt. The system is then relaxed for  $10^6$  Monte Carlo steps (MCS). This corresponds to several relaxation times of the polymer chains. After that the  $n_h$  chains with length  $N_h$  are separated into two groups according to the position of

their center of mass  $z_{cm}$ : the chains with  $z_{cm} < D/2$  are assigned as A-type and the chains with  $z_{cm} > D/2$  are assigned as B type. At the same time, the  $n_c$  chains with length  $N$  are assigned a random AB monomer sequence. The interaction between A and B species is then turned on and the system is then relaxed again for  $10^7$  MCS so that the interface (and its periodic image) between the both bulk phases is built up. The bulk phases have the perpendicular extension of more than 5 times the radius of gyration of bulk chains and more than 3 times the radius of gyration of the longest copolymer chains considered ( $N = 128$ ). This ensures that we have true bulk phases. The system is in equilibrium already after  $10^6$  MCS, so that the configurations between the  $10^6$ th and the  $10^7$ th MCS are used for calculating averages. Since the configurations were stored every  $10^4$ th MCS.

Our simulation procedure obviously ensures that the positions of RCP are randomly distributed in the simulation volume, before the interaction is turned on and the interface is built up. The random copolymers thus can choose the state which they thermodynamically prefer without being restricted to a distinguished initial state.

### 3 Results

#### 3.1 Density and radius of gyration profiles

We define first the density  $\rho_m(x, y, z)$  for a certain monomer group  $m$  by

$$\rho_m(x, y, z) = \langle n_m(x, y, z) \rangle, \quad (4)$$

where the occupation number  $n_m(x, y, z) = 1$  if there is a monomer from group  $m$  occupying the lattice position  $(x, y, z)$  and  $n_m(x, y, z) = 0$  otherwise. Because the system is homogeneous in  $xy$ -direction we consider the laterally averaged density profiles given by

$$\rho_m(z) = \frac{1}{L^2} \sum_{x,y} \rho_m(x, y, z). \quad (5)$$

Figure 1 shows the results for  $\rho_m(z)$  for different monomer groups (total bulk monomers, bulk A and B monomers and total RCP monomers) normalized by the bulk density  $\rho_b = 1/16$ . The total density of random copolymers (solid lines) exhibits pronounced peaks at both A-B interfaces. Away from the A-B interfaces, the RCP monomer density becomes almost zero. This shows that the vast majority of the random copolymers is localized at the A-B interfaces after relaxation. The total bulk density (dotted lines) exhibits a dip at the interfaces, which becomes more pronounced with increasing copolymer amount as the bulk chains more and more get expelled by the copolymers in the interface region.

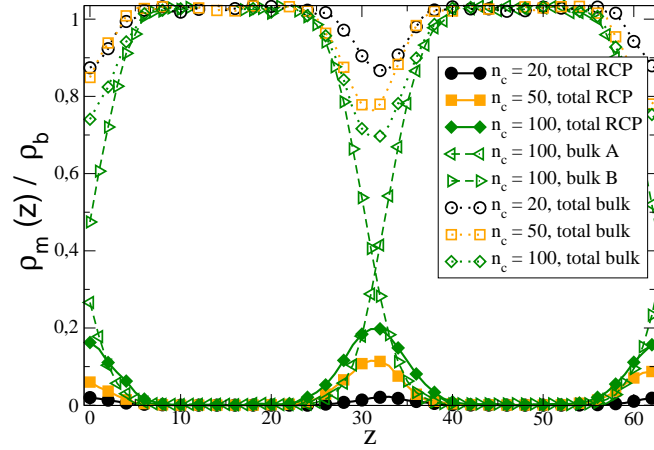


Figure 1: Perpendicular monomer density profiles  $\rho_m(z)$  normalized by the bulk density  $\rho_b = 1/16$  for different groups of monomers and different amount of copolymers  $n_c$  as indicated,  $N = 64$  and  $\varepsilon = 0.4$  ( $\chi \approx 2.8$ ).

Next we consider the perpendicular and parallel components of the squared radius of gyration defined by

$$R_{g\perp}^2 = \frac{1}{N} \sum_{i=1}^N \langle (z_i - z_{cm})^2 \rangle, \quad (6)$$

$$R_{g\parallel}^2 = \frac{1}{N} \sum_{i=1}^N \langle (x_i - x_{cm})^2 + (y_i - y_{cm})^2 \rangle, \quad (7)$$

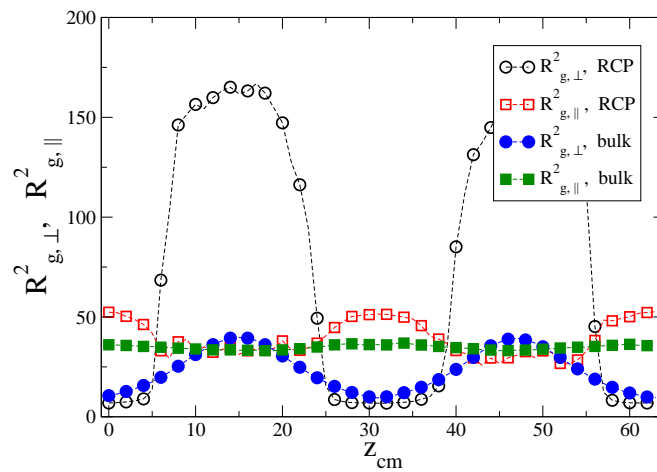


Figure 2: Perpendicular and parallel components of the squared radius of gyration vs. the  $z$  component of the chain center of mass for the copolymers and bulk chains for  $N = 64$ ,  $n_c = 200$  and  $\varepsilon = 0.4$  ( $\chi \approx 2.8$ ).

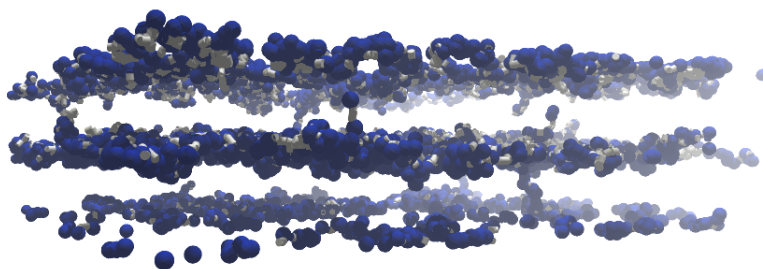


Figure 3: A simulation snapshot for the same parameter values as in Figure 2.

where  $(x_i, y_i, z_i)$  denote the position of the monomer  $i$  on the lattice and  $N$  is the total number of monomers in the polymer chain. In Figure 2 we plot  $R_{g\perp}^2$  and  $R_{g\parallel}^2$  for homopolymers and copolymers as function of the  $z$  coordinate of their center of mass  $z_{cm} = 1/N \sum_{i=1}^N z_i$ . This yields a profile for the chain extension in the direction perpendicular to the interface. We see that RCP at the interfaces are strongly squeezed in this direction. At the same time, the lateral extension of the random copolymers at the interface is greater than in the bulk. Both effects originate from the confinement of random copolymers at the interface.

As was seen from Figure 1, almost all of the random copolymers are located at the interfaces. Data points in Figure 2 indicate that a finite probability to find the center of mass of a random copolymer between the interfaces still exists. These chains are highly stretched, as compared to the bulk homopolymers. In Figure 3 a simulation snapshot for the same parameter values as in Figure 2 is shown. We see that random copolymers always have monomers at least at one of the both interfaces. Sometimes the copolymers have monomers at both interfaces so that they bridge them<sup>23</sup>. This explains the high stretching of the chains with the center of mass between the interfaces. Note the very low occurrence of these events from Figure 1.

Homopolymer chains are squeezed at the interface, too. For the parallel direction, however, no significant difference in the extension in the bulk- and the interface regions is observed for the homopolymers. This is in accordance with Silberberg's argument for melt polymers at a repulsive interface<sup>31</sup>.

Since in the initial configuration the random A-B monomer sequence were assigned to randomly chosen chains, not necessarily located at the A-B interface, from the findings of this section we already conclude that random copolymers tend to localize at the A-B interface spontaneously and independent of their initial position.

### 3.2 Interface tension

Adsorption of copolymers at the A/B interface leads to the reduction of the interface tension. The direct calculation of the interface tension from thermodynamic relations requires the access to the

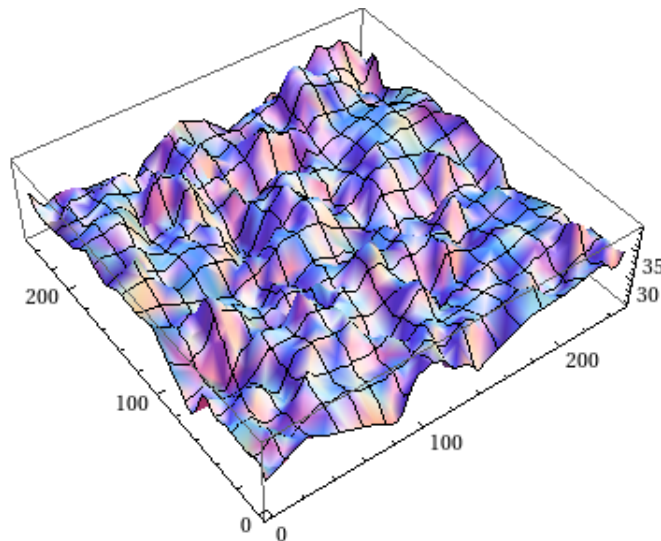


Figure 4: Snapshot of the interface calculated with block size  $B = 8$  as discussed in the text.

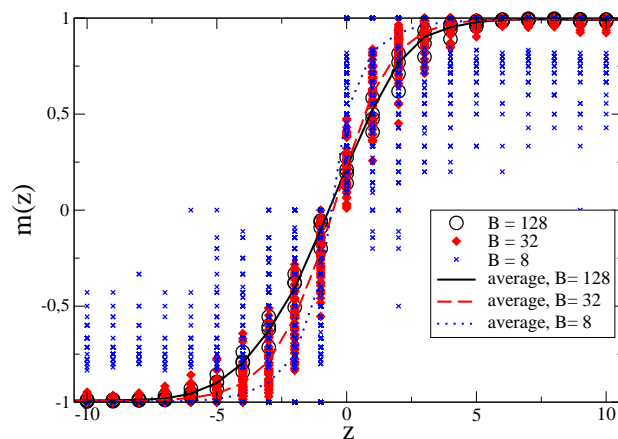


Figure 5: Density order parameter from Equation (8) for blocks of different size  $B$  with respect to the interface position in the block. The scattered data indicate the results for individual blocks. The continuous lines are averages over all blocks of a given size. With decreasing block size, the slope increases.

entropy of the system which is not directly possible from particle-based simulations. We thus apply the method of Ref.<sup>32</sup> to extract the surface tension from the broadening of the interface profile due to capillary waves. To this end, we divide the  $x - y$  plane into adjacent square blocks of size  $B \times B$  and calculate the density order parameter profiles  $m_{\mathcal{B}}(z)$  in each block  $\mathcal{B}$ :

$$m_{\mathcal{B}}(z) = \frac{1}{B^2} \sum_{(x,y) \in \mathcal{B}} \frac{\rho_A(x,y,z) - \rho_B(x,y,z)}{\rho_A(x,y,z) + \rho_B(x,y,z)}. \quad (8)$$

After that, we determine the interface position  $z_{int}(\mathcal{B})$  in each block as the  $z$  point at which the order parameter from Equation (8) changes from the negative to the positive value. A snapshot of the resulting interface profile is shown in Figure 4. The order parameter  $m_{\mathcal{B}}(z - z_{int}(\mathcal{B}))$  for individual blocks and the averaged value over all blocks of a given size  $B$

$$m(z) = \langle m_{\mathcal{B}}(z - z_{int}(\mathcal{B})) \rangle_{\mathcal{B} \in \text{blocks of size } B} \quad (9)$$

is displayed in Figure 5 as function of  $z$ . From the averaged profiles we can already see that the effective interface width is increasing with the block size. The width  $w$  of the averaged order parameter profile  $m(z)$  is fitted according to the expression from the self-consistent field theory:

$$m(z) = \tanh\left(\frac{z - z_{int}}{w}\right). \quad (10)$$

It is now important to distinguish between the intrinsic width of the interface,  $w_0$ , and interface width due to so-called capillary waves<sup>33</sup>. The averaged order parameter profile includes both contributions and leads to a large effective width  $w$ . As follows from the consideration of the interface hamiltonian<sup>34</sup>, which can be diagonalized in the Fourier space, the effect of the interface fluctuations on the effective width is described by

$$w^2 = w_0^2 + \frac{1}{4\sigma} \ln \frac{q_{max}}{q_{min}}, \quad (11)$$

where  $\sigma$  is the interface tension,  $q_{max}$  and  $q_{min}$  is the upper and the lower cutoff wave vector, respectively. Since  $B$  is the largest length scale in the block of size  $B$ , the lower cutoff  $q_{min}$  scales like  $1/B$ . The interface tension  $\sigma$  can be extracted from the slope of  $w^2$  vs.  $\ln(B)$ . In Figure 6 we plot the squared effective width,  $w^2$ , semi-logarithmically as function of the block size,  $B$ . Due to boundary effects for small and large values of  $B$ , only for the intermediate values of  $B = 16, 32, 64$  the linear scaling of  $w^2$  with  $\ln(B)$ , predicted by Equation (11) can be approximately observed. The increasing slope of the curves in this region with increasing  $n_c$  thus leads to decreasing values of  $\sigma$ .

Another way to determine the interface tension is to consider the probability distribution  $P(z)$  of the interface positions  $z_{int}(\mathcal{B})$  in the blocks, which is predicted to be Gaussian<sup>34</sup>:

$$P(z) = \frac{1}{\sqrt{2\pi s^2}} \exp\left(-\frac{z^2}{2s^2}\right) \quad (12)$$

with the variance

$$s^2 = \frac{k_B T}{2\pi\sigma} \ln \frac{q_{max}}{q_{min}}. \quad (13)$$

Figure 7 shows the interface position distributions for the pure AB interface. From the Gaussian fits (dashed lines), the variance  $s$  can be found and with the cutoff values  $q_{max} = 2\pi/B$  and  $q_{min} = 2\pi/L$ , the interface tension can be determined.

Figure 8 shows the results for the interface tension determined by both methods described above for the pure A/B interface. For the interface without copolymers, the scaling with  $\chi^{1/2}$ , expected from the strong segregation limit of the self-consistent field theory<sup>35</sup> is roughly fulfilled for larger values of  $\chi$ . The notable difference between the values of the interface tension determined by different methods in Figure 8 is well known from previous works<sup>32</sup>. We note that both methods map the real two-phase interface into a simplified model<sup>32-34</sup> with idealized zero interface thickness. Therefore, the absolute values of the surface tension calculated with both methods should be considered as model dependent. In the following we will discuss results for both methods.

In Figure 9 we plot the interface tension for interfaces with adsorbed copolymers as function

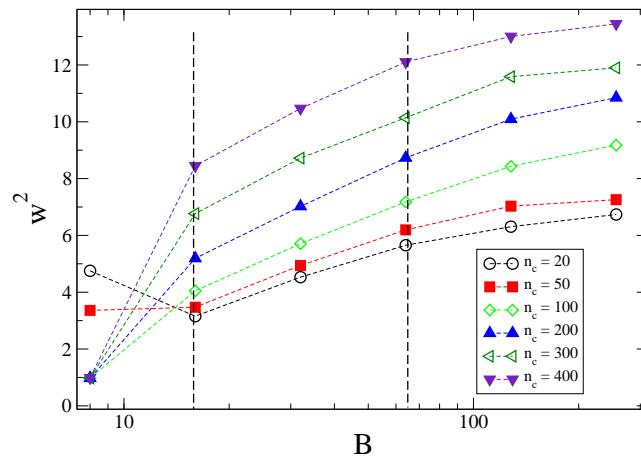


Figure 6: Squared interface width  $w^2$  vs. block size  $B$  for  $\varepsilon = 0.4$  ( $\chi \approx 2.8$ ),  $N = 64$  and different amount of copolymer chains  $n_c$  as indicated. The vertical dashed lines mark the region of the values of  $B$ ,  $16 \leq B \leq 64$ , for which the linear scaling of  $w^2$  with  $\ln(B)$  predicted by Equation (11) is observed.

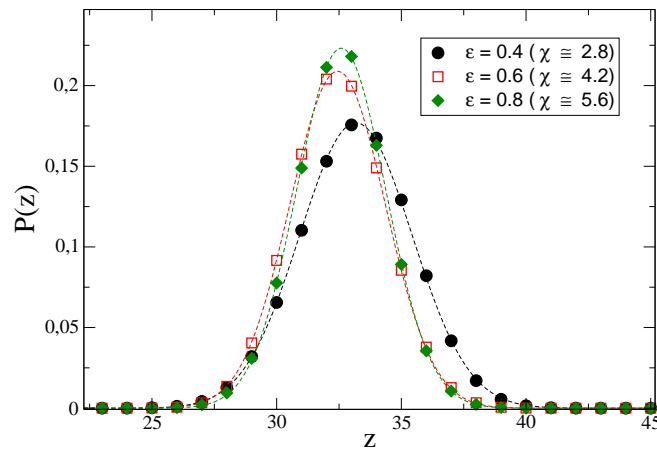


Figure 7: Distribution of interface positions for block size  $B = 8$ . The dashed lines are Gaussian fits.

of the amount of the copolymers. As can be seen, the adsorption of copolymers reduces the interface tension  $\sigma$ . A simple scaling argument in the framework of the excess blob picture (see next Section) can be used to estimate the reduction of the interface tension  $\Delta\sigma$ . A single excess blob at the interface leads to  $\Delta\sigma \sim k_B T$ . The number of excess blobs in the chain is given by  $N/g$ , where the blob size  $g$  scales as  $g \sim \chi^{-2}$ , see Equation (17). This yields

$$\Delta\sigma \sim -\frac{n_{int} N \chi^2}{L^2}, \quad (14)$$

where  $n_{int}$  is the number of chains at the interface and  $L^2$  is the interface area. In Figure 10 we plot the interface coverage  $n_{int}$  (for the same values of  $\chi$  and  $N$  as in Figure 9), the values of  $\sigma$  obtained in the simulation and the values of  $\sigma$  calculated from the above scaling relation according to

$$\sigma(\chi, n_c) = \sigma(\chi, 0) - \alpha \frac{n_{int}(\chi, n_c) N \chi^2}{L^2}. \quad (15)$$

The numerical value  $\alpha = 2.5 \times 10^{-2}$  of the prefactor was chosen as the best fit using the data with  $\varepsilon = 0.5$  ( $\chi \approx 3.5$ ).

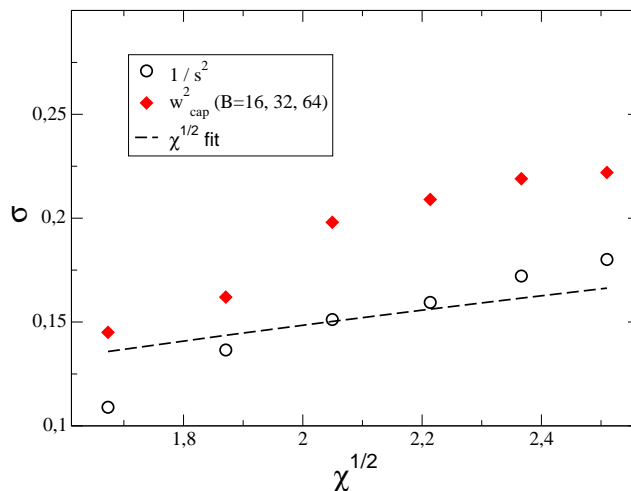


Figure 8: Interface tension of a pure A/B interface. Circles are the results from the method of interface width scaling (see Figure 6), where the values of  $B = 16, 32, 64$  were used and diamonds are the results from the method of the width of the interface position distribution (see Figure 7). The dashed line is a linear fit according to the prediction of the strong segregation model to the results from the width of the interface positions distribution.

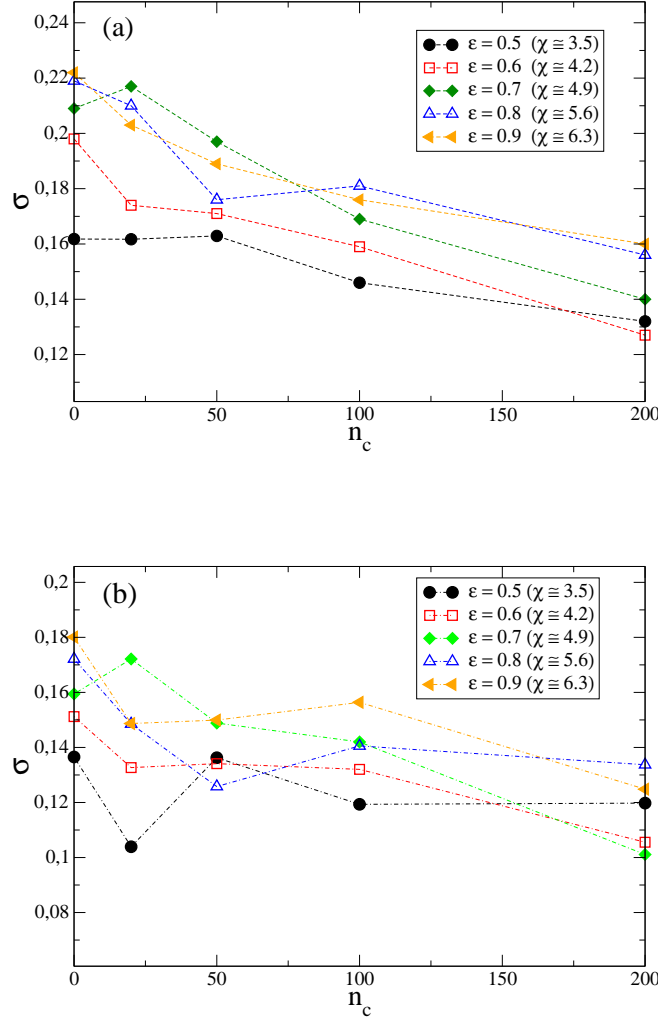


Figure 9: The interface tension as function of the amount of the copolymers  $n_c$  for  $N = 64$  and different interaction strengths  $\epsilon$ , obtained by the method of interface width scaling (a) and by the method of interface position distribution (b).

### 3.3 Scaling and excess blobs

After we have shown that the copolymer chains localize at the interface, we turn to the detailed study of their properties. The question of interest is the scaling with the relevant parameters  $\chi$  and  $N$ . It was shown for ideal interfaces<sup>7,16,18</sup> that the adsorption of single chains is controlled by the scaling variable

$$y = \chi N^{1/2}, \quad (16)$$

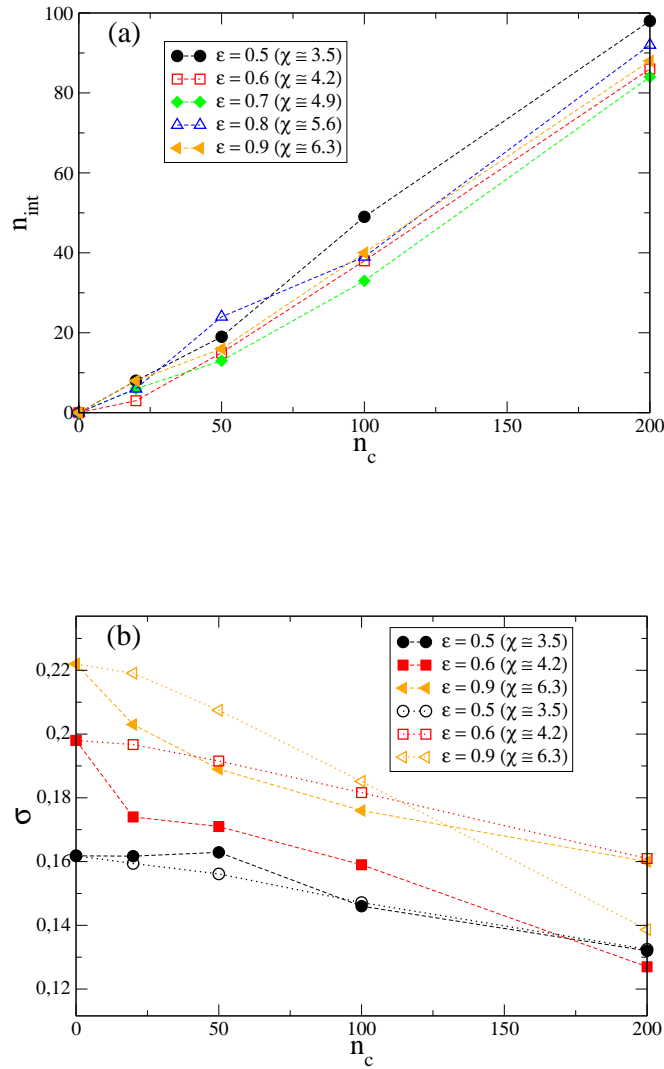


Figure 10: (a): the interface coverage  $n_{int}$  by copolymers, (b): the interface tension obtained by the method of interface width scaling (full symbols) and from the theoretical estimate according to Equation (14) (open symbols) as explained in the text. The results are displayed as function of the amount of the copolymers  $n_c$  for  $N = 64$  and different interaction strengths  $\epsilon$  as indicated.

accounting for the formation of “excess” blobs. These result from the average excess  $g^{1/2}$  of one species in a random binary sequence of  $g$  monomers. The average number of monomers  $g$  forming an excess blob should obey the following condition

$$g^{1/2}\chi \sim 1. \quad (17)$$

Blobs of this size stick to the preferred side of the selective interface because the free energy effort to enter the other side of the interface is of the order  $k_B T$ . The scaling variable which controls the localization of RCP at a selective interface is given by the number of excess blobs per chain and can be chosen as in Equation (16).

This in turn allows to derive the scaling laws for the radius of gyration of RCP at ideal interfaces. To this end, we write the perpendicular and parallel components of the radius of gyration as

$$R_{g\parallel,\perp}(\chi, N) = R_g(0, N) f_{\parallel,\perp}(y) \quad (18)$$

where  $R_g(0, N)$  is the radius of gyration for the chain of length  $N$  in the isotropic case ( $\chi = 0$ ) and  $f_{\parallel,\perp}$  are the scaling functions for the parallel and the perpendicular directions, respectively.  $R_g(0, N)$  scales according to  $R_g(0, N) \sim N^\nu$ , with the Flory exponent  $\nu = 0.588$  for excluded volume chains and  $\nu = 0.5$  for ideal chains. For  $y \ll 1$ , both scaling functions obviously should obey the asymptotic limit  $f_{\parallel,\perp}(y \ll 1) = 1$ . To determine the asymptotic limit for  $y \gg 1$ , for the perpendicular direction one employs the fact that the size of the chain is given by the blob size and does not depend on  $N$ ,  $R_{g\perp} \sim N^0$ . Assuming an asymptotic power law  $f_{\perp}(y \gg 1) = y^{m_{\perp}}$ , gives thus the relation  $\nu + m_{\perp}/2 = 0$  which leads to<sup>16,18</sup>

$$m_{\perp} = -2\nu. \quad (19)$$

As for the parallel direction, since the chains become localized around the interface and since the data suggests some swelling, as a first approximation one can consider a two dimensional chain

with excluded volume,  $R_{g\parallel} \sim N^{3/4}$  (this point will be discussed later). This leads to the relation  $\nu + m_{\parallel}/2 = 3/4$ , which gives

$$m_{\parallel} = 2\left(\frac{3}{4} - \nu\right). \quad (20)$$

The asymptotic limits for both directions can be summarized by the following equation

$$f_{\perp,\parallel}(y) = \begin{cases} 1, & y \ll 1 \\ y^{m_{\perp,\parallel}}, & y \gg 1 \end{cases} \quad (21)$$

In Figure 11, we plot  $R_{g\perp}(\chi, N)/R_g(0, N)$  and  $R_{g\parallel}(\chi, N)/R_g(0, N)$  for the copolymer chains with different length  $N$  located at the interface. As chains at the interface we define those with the center of mass within the interval  $(z_{int} - 5, z_{int} + 5)$ . We performed extra simulations of few chains of size  $N$  in the bulk of homopolymer chains at  $\chi = 0$  to determine  $R_g(0, N)$ . This was done to account for possible size effects. The results are given by  $R_g^2(\chi = 0) = 7.6, 16.2, 34.0, 69.7$  for  $N = 16, 32, 64, 128$  respectively.

For a dense melt, the Flory exponent is  $\nu = 0.5$ . Thus, we obtain in the limit  $y \gg 1$  from Equations (19) to (21),  $R_{g\perp} \sim y^{-1}$  and  $R_{g\parallel} \sim y^{0.5}$ . The subtle point here is that the copolymer chains experience some excluded volume interactions in the interface region due to the dilution of monomers. While the excess blob scaling works well for  $R_{g\parallel}$ , see Figure 11 (b), the exponent of 0.5 is only approached in the limit of very strong segregation, where the copolymer chain is nearly flatly confined in the depleted zone of the interface. On the other hand, if the copolymers would not experience any excluded volume in the interface zone, their lateral extension would not change, as for the case of bulk chains, in marked contrast to the observation in Figure 2. For the perpendicular extension, see Figure 11 (a), neither the scaling is displayed nor the expected asymptotic behavior is shown. We see that the scaling prediction  $R_{g\perp} \sim y^{-1}$  (see dashed line in Figure 11) largely overestimates the tendency for RCP to squeeze in perpendicular direction. This may be related to the fact that the interface position  $z(x, y)$  fluctuates, which overlays the measurement of the the extension of the localized copolymers in perpendicular direction.

On order to eliminate the effect of interface fluctuations we can calculate the perpendicular extension of the copolymers locally in the blocks which we already introduced for determining the surface tension in Section 3.2. Here we consider the second moment of the copolymer density distribution relative to the interface position in every block  $\mathcal{B}$  and average over all blocks of a given size:

$$D^2 = \left\langle \overline{(z - z_{int}(\mathcal{B}))^2 \rho_m(x, y, z)}_{(x, y, z) \in \mathcal{B}} \right\rangle_{\mathcal{B} \in \text{blocks of size B}} \quad (22)$$

In Figure 12 we plot  $D/N^{1/2}$  as a function of the ideal scaling variable. In fact, the scaling prediction for ideal interfaces is recovered. We note that the crossover value of  $\chi N^{1/2}$ , which is necessary to reach the asymptotic behavior is of the order unity.

The order parameter which characterizes the adsorbed state can be defined as<sup>22</sup>

$$m = \frac{2M}{N} - 1, \quad (23)$$

where  $M$  is the number of monomers in contact with their own phase. For the disordered phase ( $\chi = 0$ ), one has on average  $M = N/2$  and thus  $m = 0$ , whereas at high values of  $\chi$ , in the perfectly ordered state, all monomers should be surrounded by their own species ( $M = N$ ) and thus  $m = 1$  should apply.

Using the excess blob picture, the number of the monomers of the "right" species in a blob of size  $g$  is given on average by  $g/2 + \alpha g^{1/2}$ , where  $\alpha$  is a numerical prefactor. Since there are  $N/g$  blobs, we obtain  $M = (N/g)(g/2 + \alpha g^{1/2})$ , and thus  $m = \alpha g^{-1/2}$ . Together with Equation (17) this yields

$$m \sim \chi. \quad (24)$$

This relation can be rewritten in terms of the scaling variable Equation (16) as

$$mN^{1/2} \sim y \quad (25)$$

In Figure 13 we plot  $mN^{1/2}$  vs the scaling variable. We can see that the scaling according to the

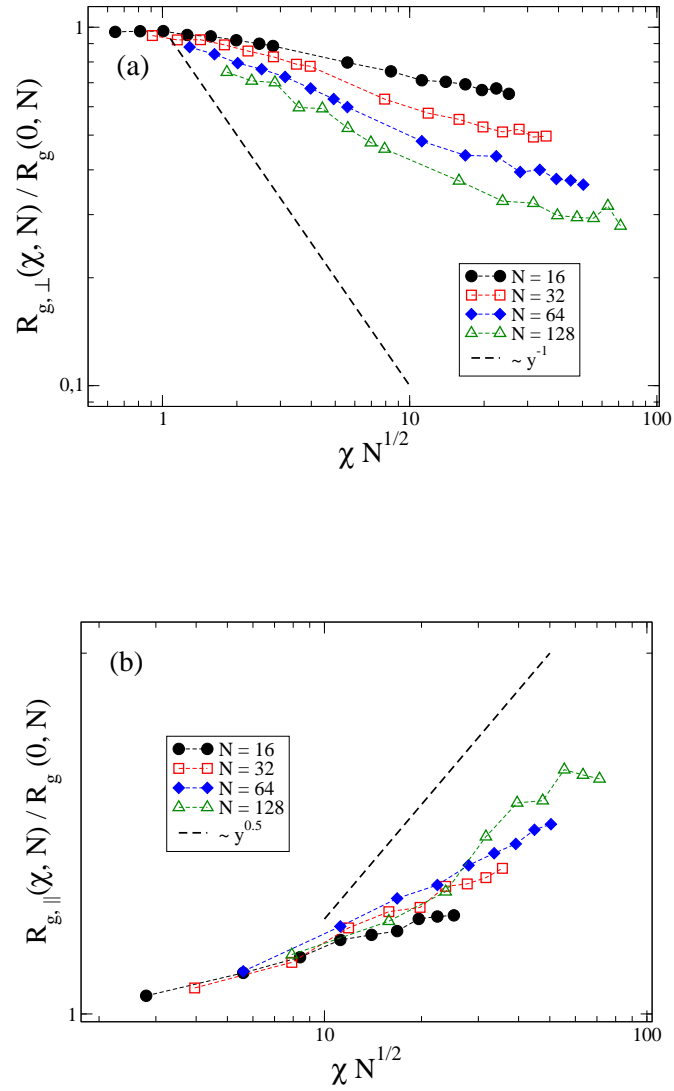


Figure 11: Squared radius of gyration perpendicular to the interface (a) and parallel to the interface (b) vs. the scaling variable Equation (16). The number of copolymers is  $n_c = 50$ .

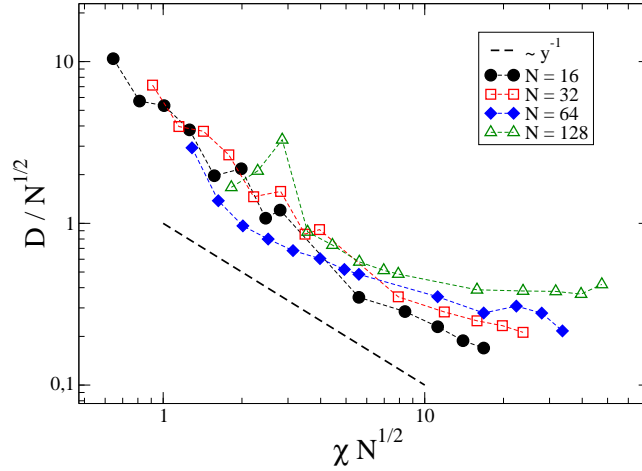


Figure 12: Square root  $D$  of the block averaged second moment of the copolymer density distribution as defined in Equation (22), scaled with the square root of the RCP length  $N$ , vs. the scaling variable. Average value over all blocks of size  $B = 16$  (see Equation (22)). The number of copolymers is  $n_c = 50$ .

above relation is fulfilled for the values of the scaling variable  $y \lesssim 10$ .

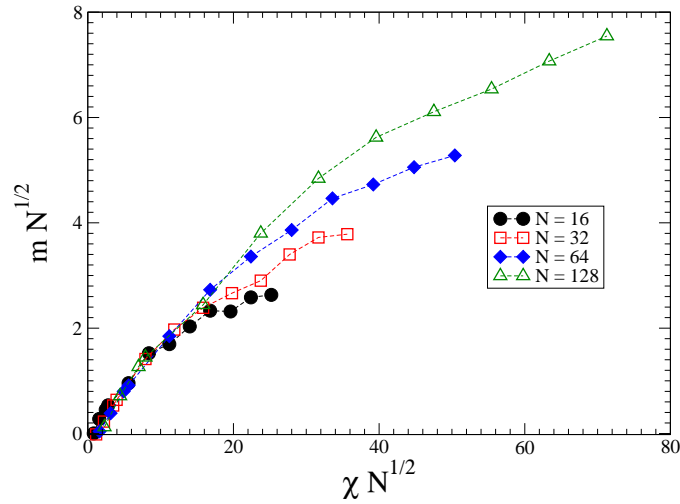


Figure 13: Rescaled order parameter as defined in Equation (25) vs. the scaling variable for  $n_c = 20$  and different  $N$ .

### 3.4 Thermodynamic considerations

Besides adsorbing at the two-phase boundary, random copolymers can reduce their free energy by forming random micelles in one of the bulk phases. It was even conjectured that the micellar

phase could have a lower free energy than the adsorbed one. Our results for the monomer density already indicate that this is not the case. In order to corroborate this finding by thermodynamic arguments, we have simulated copolymers in the single (A) phase surrounding and have calculated the potential energy of the chains

$$U = \chi \sum_{i=1}^N n_{AB}(i). \quad (26)$$

Here  $n_{AB}(i)$  denotes the number of opposite species contacts of monomer  $i$ .

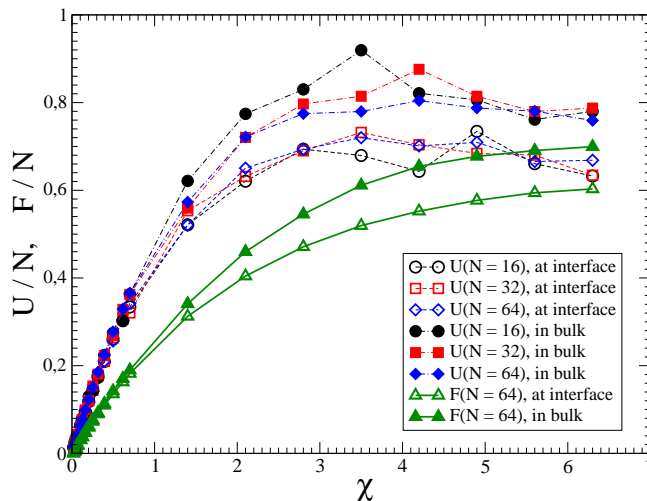


Figure 14: The potential energy and the free energy per monomer of the copolymers at the interface (open symbols) and in the bulk (full symbols) for  $n_c = 20$  and different  $N$ .

In Figure 14 we display the results for the potential energy per monomer for the random copolymers at the interface (open symbols) and in the pure bulk (full symbols). The potential energy approximately scales with the chain length in both cases. Even though in the bulk the copolymers indeed reduce their energy by micellization, the chain energy at the interface is still smaller and thus the latter case is energetically more advantageous.

In order to obtain also the free energies, we simulate the values of  $\chi$  down to the demixing threshold ( $\chi_c \approx 2/N_h = 0.031$ ) and exploit the thermodynamic integration procedure<sup>36</sup>

$$F(\beta) = \frac{1}{\beta} \int_0^\beta U(\beta') d\beta', \quad (27)$$

using the fact that  $\beta = 1/k_B T$  can be identified with the interaction parameter  $\varepsilon$  in our Monte-Carlo method. The results are represented by continuous lines on Figure 14 and show that interface adsorption is clearly more favorable than bulk micellization, not only energetically but also thermodynamically.

## 4 Conclusions

The localization of random copolymers (RCP) became a question of debate due to the possibility of micellization of the copolymers in one-phase surrounding. The previous studies of ideal interfaces could not discuss the polymers in one phase and thus could not account for the micellization effect.

Going beyond previous work we have simulated random copolymers in an explicit, strongly separated two-phase surrounding. We note that our simulations also take into account the roughness and thermal fluctuations of the interface between two homopolymer phases.

The results from the monomer density distributions already signalize that random copolymers are located at the interfaces and their appearance in the bulk is negligible (except for the very rare cases where a copolymer is anchored at both the interface and its periodic image). This means that RCP finally adsorb at the interface between the two immiscible phases, regardless of their initial position.

Using the method of the interfacial capillary waves hamiltonian, we calculated the reduction of the interface tension due to adsorption of the copolymers and compared it with a simple scaling prediction. We also checked the scaling predictions for extensional properties of random copolymers from the ideal interface studies (excess blob picture) and have shown that after appropriate corrections (accounting for the non-flatness of the interface) the scaling arguments can be applied also for fluctuating interfaces. At this point it is interesting to note that the copolymer chains display a stretching in the direction parallel to the interface which can only be explained by an residual excluded volume effect. Although the asymptotic exponent which corresponds to a crossover from Gaussian to 2D excluded volume conformation statistics is not reached, excess blob scaling is

satisfied. It remains an interesting question whether this behavior is due to the reduced density and enhanced end-point concentration in the interface region or related to corrections to excluded volume screening as proposed recently<sup>37</sup>.

To verify that the adsorbed state of the copolymers is thermodynamically stable, we have also simulated random copolymers in a one-phase bulk and compared their free energy with that of random copolymers at the two-phase boundary. We observe that even though the micellization of RCP indeed leads to energy reduction, the adsorption at the two-phase interface displays the lower free energy and is thus thermodynamically stable.

A more detailed study of random A-B micelles in pure homopolymer environment would be of interest for future studies. Also the kinetical properties of the copolymers would be of interest. Since the center of mass of an adsorbed copolymer experiences a randomly fluctuating force, a significant slowing down of the dynamics can be expected<sup>38,39</sup>.

## 5 Acknowledgments

The financial support from the European Union (ERDF) and the Free State of Saxony via TP A2 ("MolDiagnostik") of the Cluster of Excellence "European Center for Emerging Materials and Processes Dresden" (ECEMP) and from the European Union within the ITN SOMATAI is gratefully acknowledged. I. G. would like to thank Marco Werner for providing his BFM simulation code and discussions.

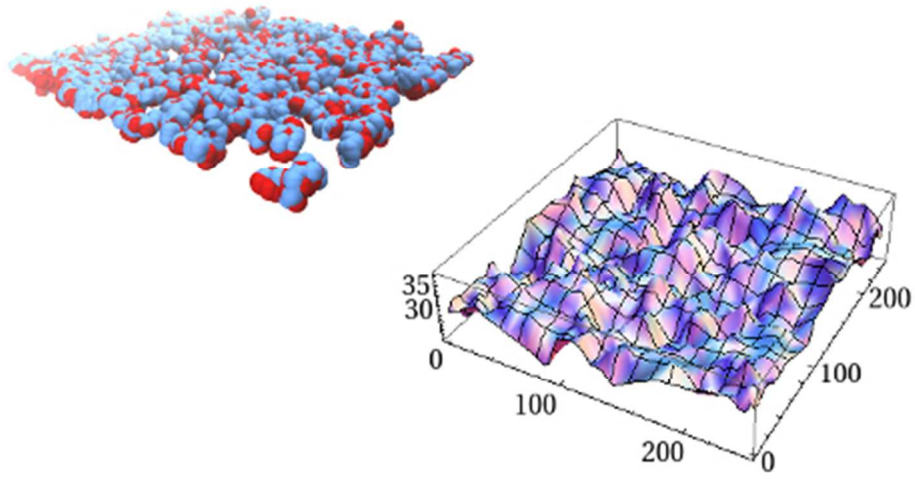
## References

- (1) Brown, H.; Deline, V.; Green, P. *Nature* **1989**, *341*, 221–222.
- (2) Dai, C.-A.; Dair, B.; Dai, K.; Ober, C.; Kramer, E.; Hui, C.-Y.; Jelinski, L. *Phys. Rev. Lett.* **1994**, *73*, 2472–2475.
- (3) Brown, H.; Char, K.; Deline, V.; Green, P. *Macromolecules* **1993**, *26*, 4155–4163.

- (4) Brown, H. *Macromolecules* **1989**, *22*, 2859–2860.
- (5) Benkoski, J. J.; Fredrickson, G. H.; Kramer, E. J. *Journal of Polymer Science Part B: Polymer Physics* **2001**, *39*, 2363–2377.
- (6) Garel, T.; Huse, D.; Leibler, S.; Orland, H. *Eur. Phys. Lett.* **1989**, *8*, 9–13.
- (7) Sommer, J.-U.; Daoud, M. *Europhys. Lett.* **1995**, *32*, 407.
- (8) Sommer, J.-U.; Daoud, M. *Phys. Rev. E* **1996**, *53*, 905–920.
- (9) Stepanow, S.; Sommer, J.-U.; Erukhimovich, I. *Phys. Rev. Lett.* **1998**, *81*, 4412–4415.
- (10) Chen, Z. Y. *J. Chem. Phys.* **2000**, *112*, 8665–8671.
- (11) Corsi, A.; Milchev, A.; Rostiashvili, V. G.; Vilgis, T. A. *The Journal of Chemical Physics* **2005**, *122*.
- (12) Corsi, A.; Milchev, A.; Rostiashvili, V. G.; Vilgis, T. A. *Journal of Polymer Science Part B: Polymer Physics* **2006**, *44*.
- (13) Corsi, A.; Milchev, A.; Rostiashvili, V. G.; Vilgis, T. A. *EPL (Europhysics Letters)* **2006**, *73*, 204.
- (14) Balazs, A.; Siemasko, C.; Lantman, C. *J. Chem. Phys.* **1991**, *94*, 1653–1663.
- (15) Yeung, C.; Balazs, A.; Jasnow, D. *Macromolecules* **1992**, *25*, 1357–1360.
- (16) Sommer, J.-U.; Peng, G.; Blumen, A. *J. Phys. II France* **1996**, *6*, 1061–1066.
- (17) Israels, R.; Jasnow, D.; Balazs, A.; Guo, L.; Krausch, G.; Sokolov, J.; Rafailovich, M. *J. Chem. Phys.* **1995**, *102*, 8149–8157.
- (18) Peng, G.; Sommer, J.-U.; Blumen, A. *Phys. Rev. E* **1996**, *53*, 5509–5512.
- (19) Werner, A.; Schmid, F.; Binder, K.; Müller, M. *Macromolecules* **1996**, *29*, 8241–8248.

- (20) Sommer, J.-U.; Peng, G.; Blumen, A. *J. Chem. Phys.* **1996**, *105*, 8376–8384.
- (21) Peng, G.; Sommer, J.-U.; Blumen, A. *Eur. Phys. J. B* **1999**, *8*, 73–79.
- (22) Klos, J.; Sommer, J.-U. *J. Chem. Phys.* **2007**, *127*, 174901.
- (23) Klos, J.; Sommer, J.-U. *J. Chem. Phys.* **2008**, *128*, 164908.
- (24) Imry, Y.; Ma, S.-K. *Phys. Rev. Lett.* **1975**, *35*, 1399–1401.
- (25) Millner, S.; Fredrickson, G. *Macromolecules* **1995**, *28*, 7953–7956.
- (26) de Gennes, P. G. *Preprint* **1995**,
- (27) Carmesin, I.; Kremer, K. *Macromolecules* **1988**, *21*, 2819–2823.
- (28) Hoffmann, A.; Sommer, J.-U.; Blumen, A. *J. Chem. Phys.* **1997**, *106*, 6709–6721.
- (29) Werner, M.; Sommer, J.-U. *Eur. Phys. J. E* **2010**, *31*, 383–392.
- (30) de Gennes, P. *Scaling Concepts in Polymer Physics*; Cornell University Press: Ithaca and London, 1979.
- (31) Silberberg, A. *J. Coll. Interface Sci.* **1982**, *90*, 86–91.
- (32) Werner, A.; Schmid, F.; Müller, M.; Binder, K. *Phys. Rev. E* **1999**, *59*, 728–738.
- (33) Müller, M.; Münster, G. *Journal of Statistical Physics* **2005**, *118*, 669–686.
- (34) Werner, A.; Schmid, F.; Müller, M.; Binder, K. *J. Chem. Phys.* **1997**, *107*, 8175–8188.
- (35) Helfand, E.; Tagami, Y. *J. Chem. Phys.* **1972**, *56*, 3592.
- (36) Binder, K. *Z. Phys. B - Condensed Matter* **1981**, *45*, 61–69.
- (37) Wittmer, J. P.; Beckrich, P.; Johner, A.; Semenov, A. N.; Obukhov, S. P.; Meyer, H.; Baschnagel, J. *EPL (Europhysics Letters)* **2007**, *77*, 56003.

- (38) Baumgartner, A.; Muthukumar, M. *The Journal of Chemical Physics* **1987**, *87*, 3082–3088.
- (39) Migliorini, G.; Rostiashvili, V.; Vilgis, T. *European Physical Journal B* **2003**, *33*, 61–73.



39x26mm (300 x 300 DPI)